Molecular Crystals and Liquid Crystals
Publication details, including instructions for authors and subscription information:
http://www.tandfonline.com/loi/gmcl20

Thermal, Spectral, and SHG Studies of 4-Piperidinium Carboxylamide Picrate Crystals

T. Dhanabal [a], G. Amirthaganesan [a], M. Dhandapani [a] & Samar K. Das [b]

[a] Department of Chemistry, Sri Ramakrishna Mission Vidyalaya College of Arts and Science, Coimbatore, Tamil Nadu, India

[b] School of Chemistry, University of Hyderabad, Hyderabad, Andhra Pradesh, India

Version of record first published: 16 Nov 2012.

To cite this article: T. Dhanabal , G. Amirthaganesan , M. Dhandapani & Samar K. Das (2012): Thermal, Spectral, and SHG Studies of 4-Piperidinium Carboxylamide Picrate Crystals, Molecular Crystals and Liquid Crystals, 569:1, 112-124

To link to this article: http://dx.doi.org/10.1080/15421406.2012.691069

Mol. Cryst. Liq. Cryst., Vol. 569: pp. 112–124, 2012

ISSN: 1542-1406 print/1563-5287 online
DOI: 10.1080/15421406.2012.691069

Taylor & Francis
Taylor & Francis Group

Thermal, Spectral, and SHG Studies of 4-Piperidinium Carboxylamide Picrate Crystals

T. DHANABAL,[1] G. AMIRTHAGANESAN,[1,*]
M. DHANDAPANI,[1] AND SAMAR K. DAS[2]

[1]Department of Chemistry, Sri Ramakrishna Mission Vidyalaya College of Arts and Science, Coimbatore, Tamil Nadu, India
[2]School of Chemistry, University of Hyderabad, Hyderabad, Andhra Pradesh, India

4-piperidinium carboxylamide picrate crystals were synthesized by slow evaporation method from a methanol solution at room temperature. The stoichiometric ratio of the complex was confirmed by elemental analysis. The ultraviolet-visible transmittance study indicates that the crystal possesses minimum transmittance at 360 nm and no absorption between 480 nm and 900 nm. The thermal analyses were used to analyze the thermal stability of the complex. The thermal anomalies observed in the cooling and heating curves of the differential scanning calorimetry indicate the occurrence of a first-order phase transition. Single crystal X-ray diffraction study reveals that the complex crystallizes in monoclinic system with space group $P2_1/c$. The various absorption bands observed in Fourier transform infrared spectral analysis were reasonably assigned. The second harmonic generation efficiency of the material was found to be five times greater than that of potassium dihydrogen phosphate.

Keywords Crystallization; differential thermal analysis; FTIR spectrum; growth from solution; phase transition; X-ray diffraction

1. Introduction

Picric acid forms crystalline picrates with various organic molecules and such picrates are convenient for identification and qualitative analysis of organic complexes [1]. The strength and nature of the electron donor–acceptor type bonding in the picric acid complexes are dictated by the nature of the partners involved in the bond formation process [2]. The linkage encompasses electrostatic interactions as well as the intermolecular interaction between picric acid and partner such as hydrogen bonding [3]. It is known that picric acid acts not only as an acceptor to form various π stacking complexes with other aromatic molecules but also as an acidic ligand to form salts through specific electrostatic or hydrogen bond interactions [4]. Bonding of picric acid as a proton donor strongly depends on the relationship of its acidity (pKa) with the basicity (pKb) of the partner. The various organic subnetworks induce noncentrosymmetry in the bulk and enhance the thermal and mechanical stabilities through hydrogen bonding interactions [5,6]. The effective nonlinear optical (NLO) single crystals

*Address correspondence to G. Amirthaganesan, Department of Chemistry, Sri Ramakrishna Mission Vidyalaya College of Arts and Science, Coimbatore 641020, Tamil Nadu, India. Tel: +91-9442002233; Fax: +91-422-2693812. E-mail: profga@yahoo.co.in

with efficient optical frequency conversion are the key elements for the development of laser systems. Such systems are of great importance as wide range tunable sources of coherent illumination in ultraviolet (UV), visible, and infrared (IR) spectral ranges. The NLO materials in their single crystal form exhibiting large optical nonlinearity are also of great interest for telecommunication, optical information processing, and high optical disk data storage [7–9]. Hence, there is a great demand to synthesize new NLO materials and grow their single crystals. Organic materials show prominent properties due to their fast and large NLO response over a broad frequency range, inherent synthetic flexibility, large optical damage threshold for laser power, and low-frequency dispersion [10,11]. Organic NLO materials are found to have high nonlinear coefficient equated to those of inorganic materials [12,13].

The aim of the present work is to synthesize and characterize the 4-piperidinium carboxylamide picrate (hereafter abbreviated as PCP) crystal showing NLO activity. The grown crystals were also characterized by elemental analysis, UV-visible analysis, thermogravimetry-differential thermal analysis (TG-DTA) and differential scanning calorimetry (DSC), single crystal X-ray diffraction method, NLO study, and Fourier transform infrared (FTIR) spectral techniques. The crystal structure of the compound was already determined at 200 K [14]. In the present work, we have determined the structure of the compound at 293 K by single crystal X-ray analysis. The second harmonic generation (SHG) efficiency of the compound is discussed in detail.

2. Experimental Details

2.1 Materials

4-piperidine carboxylamide and picric acid of the analytical grades were purchased from Sigma Aldrich (Hyderabad, India) and used without further purification. The solvent methanol used is High Pressure Liquid Chromatography (HPLC) grade.

2.2 Synthesis of PCP Crystals

Single crystals of PCP were grown by slow evaporation method from a methanol solution at room temperature. One mole of 4-piperidine carboxylamide and one mole of picric acid reacted to form PCP crystals. Methanolic solutions containing one mole of each substance were prepared separately. The synthetic procedure of PCP is shown in Scheme 1. The two solutions were mixed together and stirred well for about 6 hours to get a homogeneous solution using a mechanical stirrer and the resulting solution was filtered through a Whatman 40 filter paper into a clean dry beaker. After filtration, the filtrate was kept in dust-free environment for crystallization. The beaker was covered by an ordinary filter paper. Care was taken to minimize the temperature gradient and mechanical shock.

Under the experimental conditions, bright, transparent, and yellow colored PCP crystals were obtained within 15–25 days with dimension of $0.7 \times 0.3 \times 0.2$ mm^3. The grown crystals were collected from the mother liquid by using well-cleaned forceps. The photograph of PCP crystal is shown in Fig. 1.

2.3 Physical Measurements

The elemental analysis of the complex was carried out using a Flash 1112 SERIES EA analyzer. TG-DTA analyses were carried out using a STA 409 PC thermal analyzer under

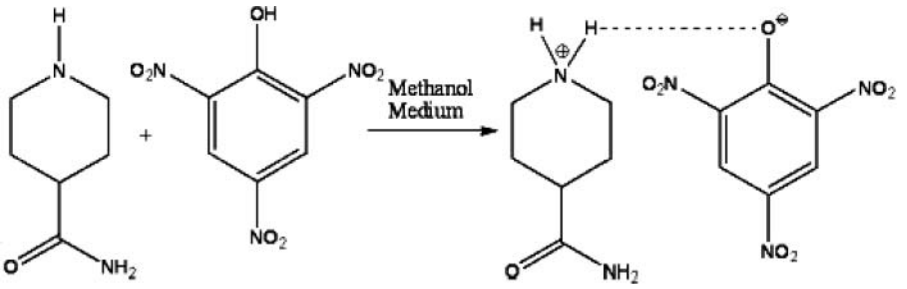

Scheme 1. Synthetic procedure of PCP.

nitrogen atmosphere. The electronic absorption spectrum of PCP was recorded using a Lambda 35 UV-visible spectrophotometer in the range of 250–900 nm. For UV-visible spectrum, the powdered complex sample was dissolved in ethanol solvent then spectrum was recorded by solution method. The low-temperature DSC of the complex was obtained using a METTLER TOLEDO instrument under nitrogen atmosphere at a heating rate of 10 K min^{-1}. The sample was cooled from 10°C to −150°C and heated back from −150°C to 10°C in the heating run. The FTIR spectrum of the complex was recorded on a JASCO-5300 FTIR spectrophotometer model instrument using KBr pellet technique at room temperature. The NLO property of the crystal was studied using Kurtz-Perry powder technique.

2.4 X-Ray Crystal Structure Determination

The crystallographic data was collected at 293 K on a Bruker SMART APEX CCD area detector system with graphite monochromator Mo Kα ($\lambda = 0.7103$ Å). A total of 2400 frames were recorded with an ω scan width of 0.3°, 10 sec exposure for each frame, crystal-detector distance 60 mm, collimator of a 0.5 mm diameter. Data reduction was performed by SAINTPLUS [15], and absorption correction was made using an empirical

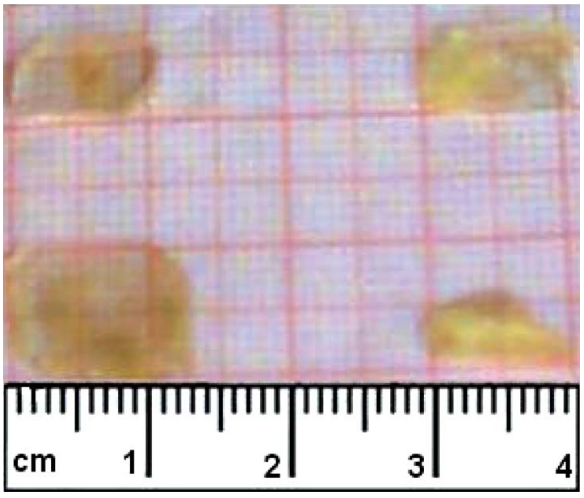

Figure 1. Photograph of PCP crystal.

method SADABS [16]. The structure solution was studied using SHELXS-97 [17] and refined using SHELXL-97 [18]. Accurate lattice parameters were determined from least square refinements of well-centered reflections in the ranges $2.91 > \theta > 26.02$. All non-hydrogen atoms were refined anisotropically. Cambridge Crystallographic Data Centre (CCDC) 838801 contains the supplementary crystallographic data for the complex. This can be obtained free of charge on application to the Director, CCDC, 12 Union Road, Cambridge CB21EZ, UK (fax: +44 1223 336 033; e-mail: deposit@ccdc.cam.ac.uk or www: http://www.ccdc.cam.ac.uk).

3. Results and Discussion

3.1 Elemental Analysis

In order to confirm the chemical composition of the synthesized complex, C, H, and N analysis was carried out. The experimental and calculated percentages of carbon, nitrogen, and hydrogen are given in Table 1. The differences between experimental and calculated percentages of carbon, nitrogen, and hydrogen are very close to each other and are within the experimental errors. This confirms the formation of the complex in the stoichiometric proportion.

3.2 UV-Visible Spectral Analysis

The UV-visible transmittance spectrum of the complex is shown in Fig. 2. From the graph, it is observed that the complex shows an absorption peak at 360 nm. There is no absorption observed between 360 nm and 900 nm in the entire visible region. Hence, the material may be useful for optoelectronic application in the region from 360 nm to 900 nm. The transmittance of the complex is due to the π-π^* transition of the constituent group. The complex has 75% transparency. The higher intensity of absorption band present in the UV region is due to the conjugated systems present in the grown material [19].

3.3 Thermal Analysis

3.3.1 TG. The TG analysis thermogram (solid line) of the complex is shown in Fig. 3. The complex is heated from room temperature to 800°C at a heating rate of 10 K min^{-1} under nitrogen atmosphere.

The complex decomposes mainly in two stages on heating between the room temperature and 430°C. The slight weight loss observed up to 115°C may possibly be due to the presence of adsorbed and occluded moisture in the crystal. The following decomposition pattern suggested explains the TGA. A weight loss of 12% occurs between 115°C and 210°C which is indicative of the loss of one molecule of NO_2 from a molecule of the complex. The calculated weight loss for this step is 12.8%. The remaining part of the molecule

Table 1. Elemental analysis data of PCP crystal

Element	Experimental (%)	Calculated (%)
Carbon	40.38	40.32
Nitrogen	19.56	19.60
Hydrogen	3.85	4.23

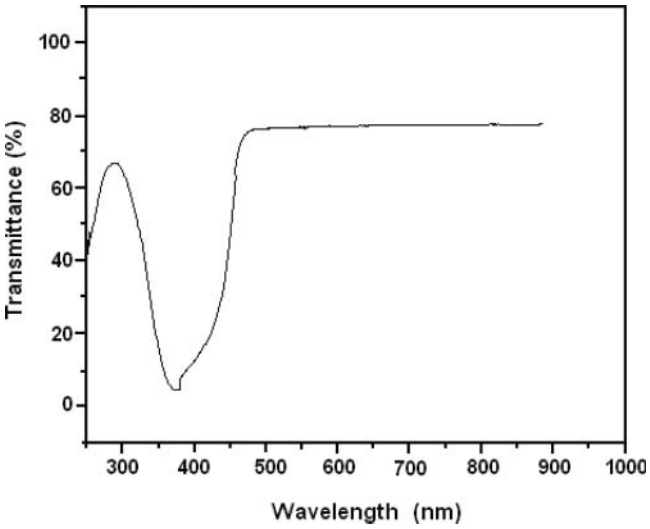

Figure 2. UV-visible spectrum of PCP crystal.

is stable up to 285°C. In the second stage, 65% weight loss occurs between 285°C and 430°C. This weight loss accounts for the removal of one molecule of NH_3, one molecule of NO_2, two molecules of CO, two molecules of NO, two molecules of hydrogen, and one molecule of 1,3-butadiene from the complex. The calculated weight loss for this step is 66.4%. The differences between the experimental and calculated weight losses in both the stages of decomposition are small and are within the experimental errors. Above 430°C, 7% of the residue was left out which is due to the charring of carbon. Thus, the TG study confirms the formation of the complex in the stoichiometric ratio. The following weight loss pattern has been suggested to account for the observed weight losses:

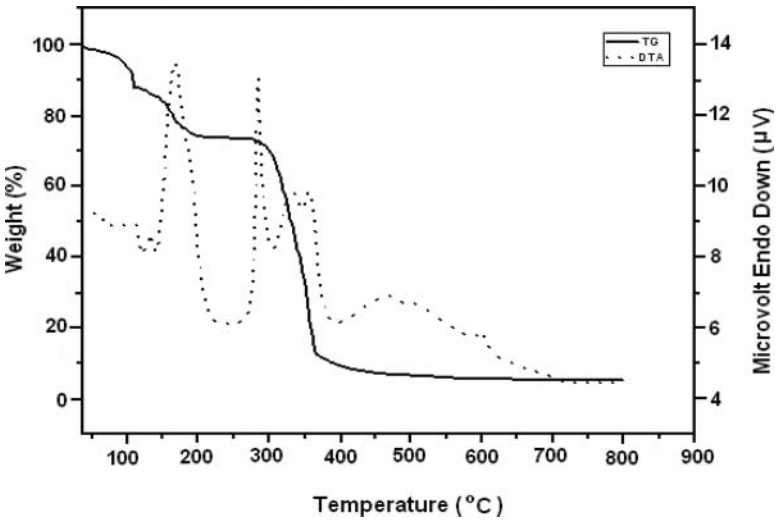

Figure 3. TG-DTA thermogram of PCP crystal.

Step 1:

$$C_{12}H_{15}N_5O_8 \xrightarrow{115^\circ C–210^\circ C} NO_2\uparrow + C_{12}H_{15}N_4O_6$$

Molecular weight: 357.29; Weight loss: 12%

Step 2:

$$C_{12}H_{15}N_3O_4 \xrightarrow{285^\circ C–430^\circ C} NO_2\uparrow + NH_3\uparrow + 2CO\uparrow + 2NO\uparrow + CH_2 = CH\text{-}CH = CH_2\uparrow + 2H_2\uparrow + C \text{ residue}$$

Weight loss: 66.4%

3.3.2 DTA. The DTA curve (dotted line) of the complex is shown in Fig. 3. There are four exothermic peaks observed. The small endothermic peak in the range of 80°C–110°C is due to the elimination of adsorbed and occluded moisture present in the crystal. The large exothermic peak at 175°C is due to melting and simultaneous first-stage decomposition of the complex. The experimental melting point of the complex is 172 ± 2°C. The sharp exothermic peak observed at 295°C and the relatively weak and broad endothermic peaks at 350°C and 480°C are due to the second-stage decomposition of the complex as described in the TG study. The DTA study conforms to TG study.

3.4 DSC Analysis

The low temperature DSC curve of the complex is shown in Fig. 4. Thermal anomalies are observed at 5°C, −115°C in the cooling cycle, and at −108°C in the heating cycle. The occurrence of thermal anomalies around −110°C associated with a thermal hysteresis in the cooling and heating cycles indicates a first-order phase transition, which may be due to ordering of 4-piperazinium carboxyalmide cation and picrate anion. First-order phase transitions are associated with thermal hysteresis.

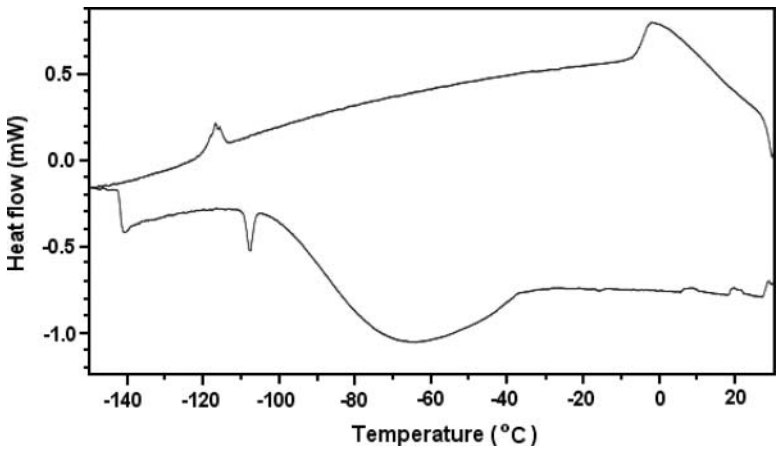

Figure 4. DSC curve of PCP crystal.

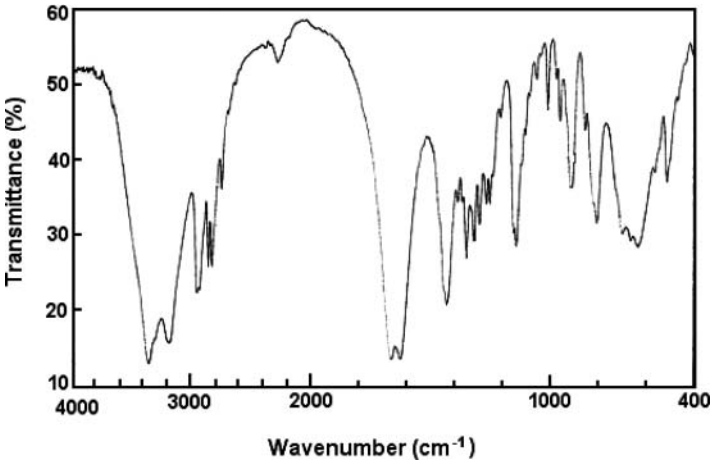

Figure 5. FTIR spectrum of PCP crystal.

3.5 FTIR Spectral Analysis

The FTIR spectrum of the complex is shown in Fig. 5. The frequency at 3352 cm^{-1} is due to the N-H asymmetric stretching vibration. The N-H symmetric stretching vibration is observed at 2950 cm^{-1}. The peaks observed at 2854 cm^{-1} and 2825 cm^{-1} are assigned to the C-H asymmetric stretching vibration in CH_2 group and C-H symmetric stretching vibration in CH_2 group is observed at 2746 cm^{-1}. The combination and overtone of NH_2 are observed at 2283 cm^{-1}. The frequencies observed at 1664 cm^{-1} and 1626 cm^{-1} are due to the presence of C=C and C=O stretching vibrations, respectively. The C-H deformation vibration in CH_2 is observed at 1433 cm^{-1}. The peak at 1305 cm^{-1} is due to C-H deformation vibration. The C-N stretching vibration of 4-piperazinium carboxyalmide cation is found at 1319 cm^{-1} and the C-N stretching vibration of picrate anion is observed at 1296 cm^{-1}. The absorption at 1267 cm^{-1} is due to the C-C stretching vibration and the NO_2 stretching vibration is observed at 1251 cm^{-1}. The frequencies at 1141 cm^{-1} and 1012 cm^{-1} are due to C-O stretching vibration. The C-H out-of-plane bending vibration is observed at 952 cm^{-1} and 910 cm^{-1}. The peaks at 856 cm^{-1} and 806 cm^{-1} are due to the CH_2 rocking vibration. The absorption at 632 cm^{-1} is characteristic of ONO stretching vibration in picrate moiety. The peak at 513 cm^{-1} is due to NO_2 rocking vibration [20].

3.6 NLO Property

The SHG efficiency of the powdered crystal was measured using Kurtz-Perry powder technique. The powdered sample was illuminated using a Q-switched Nd:YAG laser pulse of an energy of 1.34 mJ sec^{-1} with a pulse width of 8 ns and a repetition rate of 10 Hz. In this method, the powdered sample of randomly oriented crystallite particles were packed in a cell by sandwiching between glass slides. The SHG was confirmed by the emission of green radiation and the parent ray (1064 nm) was filtered using an IR filter. The amplitude of the SHG output voltage was measured using a photomultiplier and a digitalizing oscilloscope assembly. The SHG efficiencies of the standard NLO material, potassium dihydrogen phosphate (KDP), and the complex were measured as 24 mV and 120 mV, respectively. It is observed that the title complex has SHG efficiency five times greater than that of

KDP. The high SHG efficiency of the crystal is due to the centrosymmetric nature of the molecule. The presence of intermolecular hydrogen bonding can extend the level of charge transfer into the supramolecular sphere owing to their electrostatic and directive nature and thereby enhancing the SHG response [21]. In the complex under study, the strong proton donor picric acid transfers a proton to the strong proton acceptor 4-piperidine carboxylamide. Intermolecular hydrogen bonding is formed between the hydrogen atom of the protonated amino group in 4-piperazinium carboxylamide and the negatively charged oxygen atom of the picrate ion. The magnitude of optical nonlinearities depends on the strength of the donor–acceptor groups. In the present case, the donor–acceptor strength would be considerably high due to the intermolecular hydrogen bonding.

It is almost a well proven fact by both theory and experiment that to possess good SHG character, a material should have a noncentrosymmetric crystalline structure. However, there are some reports available in the literature establishing the fact that the centrosymmetric crystals [22–24] can also exhibit NLO properties. A centrosymmetric crystal can be made into a SHG active material when it possesses zero defects.

Ghazaryan et al. [25] have reported that the SHG effect for the centrosymmetrical species of diglycine picrate results from impurities of picric acid. The presence of intermolecular hydrogen bonding interactions in PCP makes it to exhibit to SHG efficiency though it is a centrosymmetric molecule.

Bhagavannarayana et al. [26] have studied the SHG efficiency of L-leucine L-leucinium picrate and found that the complex has SHG efficiency 1.5 times greater than that of KDP. The asymmetric unit of the L-leucine L-lecinium picrate contains two deprotonated leucine residues, two protonated leucinium cations, and two picrate anions.

The most important feature of this structure is the existence of a hydrogen-bonded assembly of a L-leucine molecule and picric acid. The structure is stabilized by extensive network of O-H···O and N-H···O hydrogen bonds. L-leucine residue connect two different picrate anions by strong N-H···O hydrogen bonds leading to infinite chains along the "*b*"-axis.

The donor picric acid and the acceptor L-leucine moieties in the crystal structure are held together by van der Waals forces. Hence, the effect of intermolecular hydrogen bonding between the phenolate ion of picric acid and the leucine leucinium residue will increase the hyperpolarizability value, which is the essential and required property for a system to exhibit SHG efficiency.

The dimethylammonium picrate exhibits SHG efficiency twice greater than that of KDP. The SHG efficiency of this complex is due to the proton donor (-OH) group in picric acid and proton acceptor amine ($-NH_2$) group in the dimethylamine chloride providing infrastructure to introduce the charge asymmetry. Anandha Babu et al. [27] have discussed that the charge asymmetry is required for second-order optical nonlinearity. The protonated dimethylammonium cation and deprotonated picrate anion are present as asymmetric environment in the crystal structure.

In the crystal structure of dimethylammonium picrate, the cations and anions are linked by strong intermolecular C-H···O and N-H···O hydrogen bonds. These hydrogen bonds in the crystal structure make the complex as supramolecular network. The proton donor and acceptor molecules of picric acid and dimethylamine moieties, respectively, are bound by van der Waals forces. Hence, the presence of intermolecular hydrogen bonding interactions between the dimethylamine and picric acid will enhance the hyperpolarizability of the complex. This is one of the reasons for a compound to exhibit SHG efficiency.

The high SHG efficiency of PCP may be due to the presence of N-H···O and C-H···O intermolecular hydrogen bonds. The C-H···O hydrogen bonds are formed between the ortho hydrogens in 4-piperidinium carboxylamide cation and oxygens in the -NO_2 groups present in the picrate ion. The high SHG efficiency of the title complex indicates that this may be used as a potential candidate for NLO material.

3.7 Single Crystal X-Ray Diffraction Method

Smith et al. have determined the structure of the compound at 200 K and the *R* factor was found to be 0.034. In the present work, the single crystal X-ray analysis was carried out at 293 K and the *R* factor was found to be 0.030 which is slightly lower than the earlier study [14]. The unit cell parameters of the crystals in both the cases (200 K and 293 K) are almost similar. The crystallographic data and structure refinement is given in Table 2. The

Table 2. Crystallographic data of PCP crystal

Empirical formula	$C_{12}H_{15}N_5O_8$
Formula weight	357.29
Temperature	293
Wavelength	0.7107 Å
Crystal system	Monoclinic
Space group	$P2_{(1)}/c$
Cell dimensions	a = 13.4619(10) Å, b = 13.7619(11) Å, c = 8.3863(7) Å, $\alpha = 90.00^\circ$, $\beta = 100.857(8)^\circ$, $\gamma = 90.00^\circ$
Volume	1525.8(2) $Å^3$
Z	4
Density (calculated)	1.555 Mg m^{-3}
Absorption coefficient	0.132 mm^{-1}
F_{000}	744
Crystal size	0.42 × 0.14 × 0.08 mm^3
Reflections collected	5873
Range for data collection (deg)	2.23°–26.00°
Number parameters	247
Absorption correction	Semiempirical from equivalents
Max. and min. transmission	0.9465 and 0.9895
Limiting indices h, k, l	−16/12, −16/13, −9/8
Refinement method	Full-matrix least squares on *F*2
Goodness-of-*t* on *F*2	1.063
Final *R* indices	$R1 = 0.0674$, w$R2 = 0.1624$
R indices (all data)	$R1 = 0.0531$, w$R2 = 0.1510$
Largest diff. peak and hole	0.411 and −0.485 e.$Å^{-3}$
Structure determination	SHELXS-97
Refinement	SHELXL-97
R_{int}	0.0304
CCDC number	838801

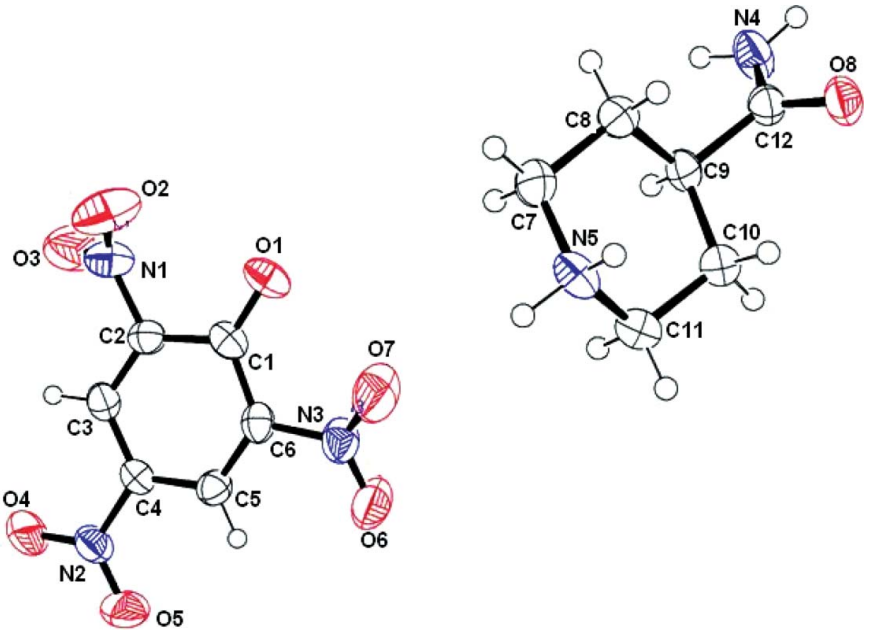

Figure 6. ORTEP diagram of PCP with 50% probability.

crystal structure of PCP was determined by SHELXS-97 and the structure was refined by using SHELXL-97.

The PCP crystal belongs to the monoclinic crystal system with space group $P2_1/c$. The ORTEP diagram of the crystal is shown in Fig. 6. The 4-piperidinium carboxylamide cation appears in crystalline lattice as single protonated cation and the picrate ion is present as deprotonated anion.

An analysis of the tilting nature of the nitro groups in picrate ion shows that the ortho groups, in general, deviate away from the benzene plane, possibly as a result of steric interactions with the phenolic oxygen atom (O1). However, the para nitro groups lies in the benzene ring. It is found that this deviation facilitates atom O4 in this group taking part in N-H···O hydrogen bond formation with the cation. Therefore, the tilting of the nitro groups is a consequence of the interactions between ions in addition to the steric repulsion with the neighboring groups.

The two-dimensional crystal packing diagram of PCP crystal is shown in Fig. 7. The packing of molecules in the lattice is determined by conventional and unconventional C-H···O hydrogen bonds. The hydrogen-bonded network of the complex clearly shows that the 4-piperidinium carboxylamide cation part is joined to the picrate anion via extensive hydrogen bonding. In addition to the conventional hydrogen bonds, the short C-H···O intramolecular contacts between C3-H3 or C5-H5 and nitro groups are observed. These hydrogen bonds are responsible for the stability of the network structure of PCP crystal. X-ray single crystal structure of the proton-transfer complex of 4-piperidine carboxylamide with picric acid shows the presence of monoprotonated 4-piperidinium carboxylamide cation and gives intermolecular hydrogen bonding associations. The hydrogen bonding parameters are presented in Table 3. The hydrogen bonding environment around each cation and anion is studied by C-H···O and N-H···O interactions and the pictures are shown

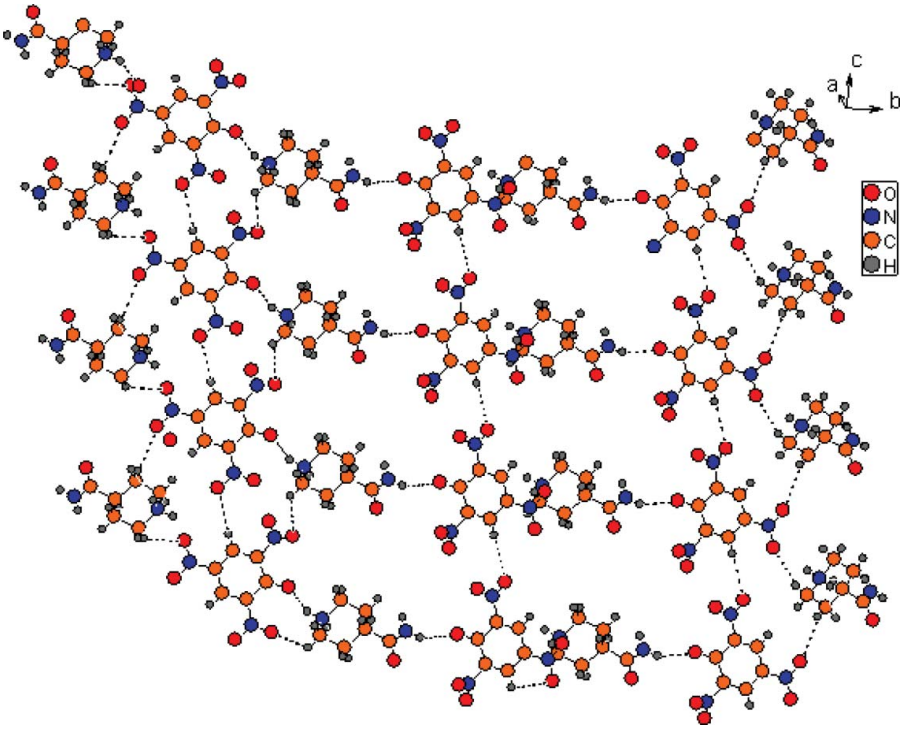

Figure 7. Two-dimensional crystal packing diagram of PCP crystal.

in Figs 8(a) and (b). In this structure, seven hydrogen bonding interactions around the cation and one hydrogen bonding interaction around the anion are observed. Symmetry transformations used to generate equivalent atoms are (1) x, y, $-1 + z$, (2) $-x$, $1 - y$, $1 - z$, (3) x, $0.5 - y$, $-0.5 + z$, (4) x, $0.5 - y$, $1.5 + z$, (5) x, $0.5 - y$, $0.5 + z$, (6) $1 - x$, $-0.5 + y$, $0.5 - z$, (7) $1 - x$, $1 - y$, $1 - z$, (8) $-x$, $-y$, $2 - z$. The combination of all types of intermolecular hydrogen bonds forms a three-dimensional network. In the crystal structure, the cations and anions are linked by strong N-H···O hydrogen bonds. The structure is

Table 3. Hydrogen bonding parameters (Å and °) of PCP crystal

D-H···A	d (D-H)	d (H···A)	d (D···A)	<(DHA)
N5-H2NB···O8	0.93 (3)	2.00 (3)	2.903 (3)	165 (3)
C11-H11A···O5	0.97	2.72	3.482 (4)	135.9
C11-H11A···O4	0.97	2.43	3.261 (3)	143.2
N5-H1NA···O1	0.94 (4)	1.88 (4)	2.746 (3)	152 (3)
C11-H11B····O2	0.97	2.72	3.429 (4)	130.4
N4-H4NA···O8	0.86 (3)	2.05 (3)	2.910 (3)	175 (3)
N4-H4NB···O1	0.85 (3)	2.38 (3)	3.085 (3)	141 (3)
C3-H3···O6	0.93	2.62	3.549 (3)	174.0
C7-H7B···O4	0.97	2.78	3.522 (4)	133.5

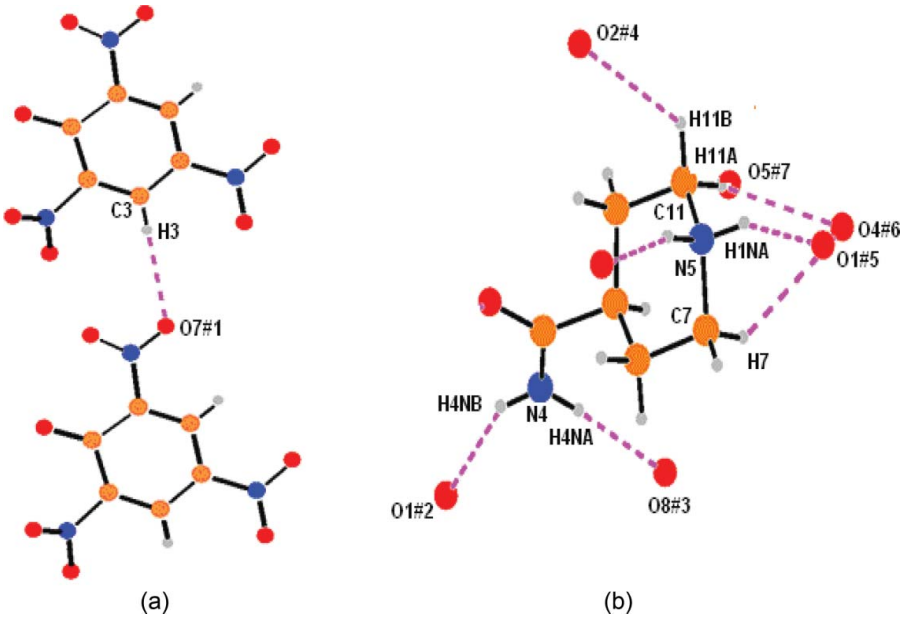

Figure 8. Hydrogen bonding environment around each anion and cation (a and b); color codes: O, red; C, magenta; N, blue; H, gray.

also stabilized by C-H···O hydrogen bonding. These hydrogen bonds link the layers of cations with the layers of anions to form a straight chain along the *b*-axis. The presence of intermolecular N-H···O and C-H···O hydrogen bonding interactions in the compound makes a supramolecular structure. These hydrogen bonds link the cations and anions layers as shown in Fig. 7. The presence of supramolecular hydrogen bonding interactions in the crystal is one of the important criteria to exhibit the SHG efficiency.

4. Conclusion

Single crystal of PCP was grown by slow evaporation method from a methanol solution at room temperature. The elemental analysis confirms the formation of the complex in a 1:1 stoichiometric ratio. The UV-visible transmission spectrum revealed the linear optical properties of the grown crystals. TG-DTA analyses were carried out to study the thermal behavior of the crystal. The thermal anomalies observed in the DSC heating and cooling cycles indicate a first-order phase transition. The FTIR spectrum characterizes the presence of various functional groups. The single crystal X-ray diffraction study indicates that the complex crystallizes in monoclinic system. The Kurtz-Perry powder SHG measurement was used to confirm the NLO property of the grown crystal and found that the complex has SHG efficiency five times greater than that of KDP.

Acknowledgments

The authors gratefully acknowledge the School of Chemistry, University of Hyderabad, Hyderabad for their instrumental facilities. One of the authors, T. Dhanabal thank the UGC-Networking Centre, School of Chemistry, University of Hyderabad, Hyderabad for

the measurement of single crystal X-ray diffraction analysis. The authors are thankful to Prof. P.K. Das, IPC, IISc Bangalore for NLO measurements.

References

[1] Takayanagi, H., Kai, T., Yamaguchi, S., Takeda, K., & Goto, M. (1996). *Chem. Pharm. Bull*., *44*, 2199.
[2] Yamaguchi, S., Goto, M., Takayanagi, H., & Ogura, H. (1988). *Bull. Chem. Soc. Jpn*., *61*, 1026.
[3] Zaderenko, P., Gel, M. S., Lopez, P., Ballesteros, P., Fonseco, I., & Albert, A. (1997). *Acta Crystallogr. B*, *53*, 961.
[4] In, Y., Nagata, H., Doi, M., Ishida, T., & Wakahara, A. (1997). *Acta Crystallogr C*, *53*, 367.
[5] Criado, A., Dianez, M. J., Garrido, S. P. L., Fernandes, I. M., Belsley, M. E., & De Gomes, M. (2000). *Acta Crystallogr. C*, *56*, 884.
[6] Zaccaro, J., Salvestrini, J. P., Ibanez, A., Ney, P., & Fontana, M. D. J. (2000). *Opt. Soc. Am.*, *17*, 427.
[7] Ledoux, I. (1993). *Synth. Metal*, *54*, 123.
[8] Yuan, D. R., Xu, D., Zhang, N., Liu, M. G., & Jiang, M. H. (1996). *Chin. Phys. Lett.*, *13*, 841.
[9] Iwai, M., Kobayashi, T., Furya, H., Mori, Y., & Sasaki, T. (1997). *J. Appl. Phys. Jpn.*, *36*, 276.
[10] Zyss, J., Nicoud, J. F., & Coquillay, M. (1984). *J. Chem. Phys.*, *81*, 4160.
[11] Ledoux, I., Badan, J., Zyss, J., Migus, A., Hulin, D., Etchepare, J., Grillon, G., & Antonetti, A. (1987). *J. Opt. Soc. Am. B*, *4*, 987.
[12] Petrosyan, H. A., Karapetyan, H. A., Antipin, M. Y., & Petrosyan, A. M. (2005). *J. Cryst. Growth*, *275*, 1919.
[13] Xue, D., & Ratajczak, H. (2005). *J. Mol. Struct. Theochem.*, *716*, 1.
[14] Smith, G., & Wermuth, U. D. (2010). *Acta Cryst. C*, *66*, 609.
[15] Sheldrick, G. M. (1998). *Software for the CCD Detector System*, Bruker Analytical X-ray Systems Inc.: Madison, WI.
[16] Sheldrick, G. M. (1996). *SADABS, A Program for Absorption Correction with the Siemens SMART Area Detector System*, University of Göttingen: Germany.
[17] Sheldrick, G. M. (1997). *SHELXS-97, A Program for Solution of Crystal Structures*, University of Göttingen: Germany.
[18] Sheldrick, G. M. (1997). *SHELXL-97, A Program for Solution of Crystal Structures*, University of Göttingen: Germany.
[19] Guru Prasad, L., Krishnakumar, V., Shanmugam, G., & Nagalakshmi, R. (2001). *Cryst. Res. Technol*., *45*, 1057.
[20] Nakamoto, K. (1978). *Infrared and Raman Spectra of Inorganic Coordination Complexes,* 3rd ed. John Wiley & Sons: New York.
[21] Natarajan, S., Umamaheswaran, M., Kalyana Sundar, J., Suresh, J., & Martin Britto Dhas, S. A. (2010). *Spectrochemica Acta Part A*, *177*, 160.
[22] Rieckhoff, K. E., & Peticolas, W. L. (1965). *Science*, *147*, 610.
[23] Ishihara, T., Koshino K., & Nakashima, H. (2003). *Phys. Rev. Lett.*, *91*, 253.
[24] Samoc, A., Samoc, M., Kolev, V. Z., & Davies, B. L. (2006). In: *Symposium on Photonics Technologies for 7th Framework Program*, Wroclaw: Woodhead Publishing Ltd., Vol. 250.
[25] Ghazaryan, V. V., Fleck, M., & Petrosyan, A. M. (2011). *Spectrochimica Acta Part A*, *78*, 128.
[26] Bhagavannarayana, G., Riscob, B., & Shakir, M. (2011). *Mat. Chem. Phys.*, *126*, 23.
[27] Anandha Babu, G., Sreedhar, S., Venugopal Rao, S., & Ramasamy P. (2010). *J. Cryst. Growth*, *312*, 1957.